



Published in final edited form as:

Nano Lett. 2010 February 10; 10(2): 398–405. doi:10.1021/nl902741x.

Anomalous Large Reactivity of Single Graphene Layers and Edges Towards Electron Transfer Chemistries

Richa Sharma, Joon Hyun Baik, Chrisantha J. Perera, and Michael S. Strano*

Department of Chemical Engineering, Massachusetts Institute of Technology, Cambridge, Massachusetts 02139

Abstract

The reactivity of graphene and its various multilayers towards electron transfer chemistries with 4-nitrobenzene diazonium tetrafluoroborate is probed by Raman spectroscopy after reaction on-chip. Single graphene sheets are found to be almost ten times more reactive than bi- or multi- layers of graphene according to the relative disorder (D) peak in the Raman spectrum examined before and after chemical reaction in water. A model whereby electron puddles that shift the Dirac point locally to values below the Fermi level is consistent with the reactivity difference. Because the chemistry at the graphene edge is important for controlling its electronic properties, particularly in ribbon form, we have developed a spectroscopic test to examine the relative reactivity of graphene edges versus the bulk. We show, for the first time, that the reactivity of edges is at least two times higher than the reactivity of the bulk single graphene sheet, as supported by electron transfer theory. These differences in electron transfer rates may be important for selecting and manipulating graphitic materials on-chip.

Introduction and Motivation

Since the first isolation of single graphene sheets in 2004¹, the material has inspired many theoretical and experimental applications due to its near-ballistic transport at room temperature and carrier mobilities as high as 200,000 cm²/Vs²⁻⁶. Recently, significant progress has been made to fabricate graphene devices i.e field-effect transistors^{7,8}, and to understand their electronic properties^{1,9,10}. However, many important issues yet need to be addressed to fully utilize the high mobility of this material. Among these are band gap engineering and controllable doping of semi-metal graphene. Chemical functionalization has been proposed by several authors as one feasible solution to these problems¹¹⁻¹⁴.

Moreover, the edges of graphene ribbons are thought to significantly influence their chemical properties and reactivity, as we have recently shown theoretically¹⁵. The non-uniformity of graphene edges and potential for dangling bonds are also issues requiring special attention¹⁶⁻¹⁸. Chemical modification of various forms of graphene including reduced graphene oxide¹⁹ and epitaxial graphene²⁰ has been previously demonstrated. However, there remains a dearth of experimental data on the chemical reactivity of pristine graphene and its multilayers. A detailed understanding of the chemical properties of

*The author to whom all correspondence should be addressed. strano@MIT.edu.

graphene is of great interest to address the above issues and to ultimately manipulate their electronic properties for different applications.

In this work we present a detailed study of the reactivity of pristine single, bi- and multi-layer graphene and also edges of single graphene sheets towards electron transfer chemistries. Our goal is to investigate the chemical properties of pristine graphene, and we therefore exclude graphene oxide from our study. This understanding may lead to specific chemistries to achieve two immediate goals of the field: (1) selective functionalization of edges exclusively and (2) the controlled and stable doping of graphene.

Experimental Method

The method employed is to prepare single and multi-layer graphene pieces from the micromechanical cleavage of bulk graphite¹ and place a solution containing various aryl diazonium reactants over it, allowing only the exposed top surface and the edges of the sheet to react and undergo electron transfer chemistry, forming a covalently bonded phenyl substituent. Figure 1 shows the schematics of this electron transfer chemistry. Pristine single and multi-layer graphene sheets are deposited by mechanical exfoliation on silicon wafers with 300nm thermal silicon dioxide. Several single and multi-layer graphene sheets are deposited on each wafer followed by annealing at 400°C for one hour. The electron transfer chemistry is then conducted on all species on the entire wafer in water with 17–25mM water soluble nitrobenzene diazonium salt (4-nitrobenzene diazonium tetrafluoroborate) obtained from Sigma Aldrich.

Each silicon wafer with the single and multi-layer graphene samples is submerged in the reactant solution for 7–12 hrs at 35–45 °C under ample stirring. In the absence of the anionic surfactant sodium dodecyl sulfate (SDS), the reaction rate appears to be negligible. To prepare the reactant solution, an aqueous solution of 1% wt SDS is added to bring the water soluble, cationic diazonium reagents in close proximity of the highly hydrophobic graphene sheets. The reactor design appears in the supplement as Figure S4. This surfactant is known to form hemi-cylindrical structures on HOPG²¹. The hydrophobic tail of the surfactant sits in the vicinity of graphene and the polar head is expected to interact with the diazonium reagent, increasing its concentration near the surface of the graphene. After 7 hours in the reactant at a temperature of 35°C, each wafer is rinsed copiously with reagent free deionized (DI) water and immersed for 5 additional hours in DI water to ensure removal of unreacted diazonium reagent on the graphene surface.

Results and Discussions

Electron transfer chemistry for single and multi-layer graphene

Interestingly, even for species present on the same wafer, we observe a substantial difference between the reaction conversion of a single sheet and its multilayer counterparts including bilayer graphene. The single sheet is far more reactive than the bi- or multi-layer. The Raman G mode corresponds to the carbon-carbon bond vibration and in the absence of resonance enhancement or formal charging, it is expected to be largely unaffected by chemical reaction as observed for carbon nanotubes²². Graphene can be identified in terms

of its number and orientation of layers by means of inelastic and elastic light scatterings, such as Raman and Rayleigh spectroscopies^{23,24}. Raman spectroscopy also has been successfully used as a highly sensitive gauge to monitor of doping, defects, strain and chemical functionalization for carbon nanotubes^{22,25–27} and graphene^{28–33}. Moreover in case of the Raman spectroscopy of graphene there is no resonant enhancement unlike carbon nanotubes. In the case of carbon nanotubes, there is a unique resonance Raman effect due to the coupling of the excitation light with a particular interband transition between van Hove singularities in the 1D electron density of states. The absence of this resonance effect for graphene greatly simplifies the interpretation of relative disorder to tangential (D/G) peak intensities in the Raman spectrum. We have asserted that the peak ratio should be uniformly related to the number of defects per area for single walled carbon nanotubes^{22,34} and we therefore use the Raman D/G ratio as a measure of the extent of chemical functionalization, as we have done previously for carbon nanotubes^{22,34}.

We observe a high density of covalent defects for single graphene sheets after reaction according to the Raman spectra collected before and after the reaction. The D/G peak ratio after reaction is almost an order of magnitude higher for a single graphene sheet than for bi- and multi- layers, even on the same reacted wafer. Figure 2a, b show the microscopic images of the single, bi- and multi- layer of graphene sheets with labels L1, L2 and L3 spots on these sheets, with the corresponding Raman spectra at 532 nm excitation in figure 2c,d,e respectively. The left spectrum in figure 2(c–e) is that of pristine graphene sheet for comparison. For these measurements the laser spot of $\sim 0.6\mu\text{m}$ diameter is focused on the central region of the sheet at least $5\mu\text{m}$ away from the edge to ensure that the signal had no edge component. The spectra on the right (labeled functionalized) are collected after the electron transfer chemistry at the identical spots as the pristine sheet controls. These locations are identified after chemistry by using the features of the graphene as distinctive microscopic markers. The D/G peak increase for single sheet (figure 2c) is almost an order of magnitude higher than for bi- (figure 2b) and multi- layer (figure 2c) graphene.

Reactivity data from more than 22 single and multi- layer graphene specimens on different silicon substrates is summarized in figure 3 and the detailed D/G ratio before normalization is included in supplement as Table T1. Slight variations in total conversion exist between graphene species on different wafers, presumably due to variations in the experimental conditions and variations in the total carbon present from wafer to wafer. To account for these variations for each silicon chip housing the graphene samples, the D/G ratio is normalized by its largest value found for a graphene sheet on the substrate. This is invariably a single layer ($N = 1$). This allows us to eliminate the differences in the extent of reaction for different substrates arising from apparently minor variations in reaction conditions and sample preparation. Note that the conclusions remain unchanged if this normalization is ignored. We express this relative reactivity ratio as $(D/G)/(D/G)_0$. A sharp decrease is clearly observed in the D/G ratio with an increase in the number of sheets from one ($N=1$) to infinite (graphite). All the spots on graphene for this analysis are defect free before reaction due to absence of D peak. Therefore the D peak after the electron transfer chemistry can be entirely attributed to the attachment of functional groups ($\text{C}_6\text{H}_5\text{-NO}_2$) to the graphene carbon atoms. Attachment of these functional groups changes the hybridization of some

graphene carbon atoms from sp² to sp³ and therefore disrupts the symmetry resulting in the disorder and (D) peak.

The simplest explanation for this inverse trend of increasing reactivity with decreasing layer number in figure 3 is that the Raman process, which necessarily samples interior carbon atoms shielded from the chemical treatment but not the scattering process, is contributing to an increasing G peak intensity for a given D band caused by functionalization of presumably only the outer layer. In the absence of resonance, the trend would then scale as $\frac{1}{N}$ where N is the layer thickness. We plot this trend in figure 3 to clearly rule out this interpretation, as the experimental diminution is obviously greater than $\frac{1}{N}$. We therefore conclude that single layer graphene sheets have higher reactivity than bi- and other multi- layers of graphene.

A more compelling observation, but one that is unsupported by the experimental data in figure 3, is that we are observing reactivity differences between single, bi- and multi- layer graphene sheets due to differences in their density of electronic states (DOS). The DOS for these structures is related to their electron transfer rates by Gerischer Marcus theory, as we have previously shown^{15,35,36}.

According to the detailed Gerischer-Marcus theory, charge transfer depends on the electronic density of states (DOS) of the reacting species and is not restricted to their Fermi levels only. The electron-transfer reaction rate (k_{ET}) is given by equation 1.1 $W_{ox}(\lambda, E)$ is the distribution of the unoccupied redox states of the electron acceptor in solution given by equation 1.2. $DOS_{Graphene(N=1/N=2)}$ is the electronic density of states of graphene for N=1, and of bilayer graphene for N=2 and ϵ_{ox} is the proportionality function.

$$k_{ET}^{GNR} = v_n \int_{E_{redox}}^{E_F^{Graphene}} \epsilon_{ox}(E) DOS_{Graphene(N=1/N=2)}(E) W_{ox}(\lambda, E) dE \quad (1.1)$$

$$W_{ox}(\lambda, E) = \frac{1}{\sqrt{4\pi kT}} \exp\left(-\frac{(\lambda - (E - E_{redox}))^2}{4\lambda kT}\right) \quad (1.2)$$

Figure S1 in the supplementary information shows the energy overlap of the electronic states of single and bilayer graphene DOS and vacant oxidation states of the electron withdrawing species (W_{ox}). This overlap directly determines the electron transfer rate from graphene and bilayer graphene to the electron-withdrawing group. Assuming ϵ_{ox} is independent of energy and ϵ_{ox} and v_n are same for graphene and bilayer graphene, they cancel out in calculations for the relative rate constants. The reorganization energy λ lies in between 0.5 and 1 eV and we use a value of 0.9. These calculations suggest bilayer graphene to be almost 1.6 times more reactive than a single layer graphene, opposite the trend of what is observed experimentally in this work.

Therefore, these electron transfer rate calculations based on DOS of pristine single layer, bilayer of graphene³⁷ and graphite³⁸ do not support the higher reactivity of single graphene sheet (figure 3). On the contrary these calculations suggest bilayer to be almost 1.6 times more reactive than a single layer.

A more plausible explanation for this enhanced electron transfer is the ionized impurities on SiO₂ substrate that can lead to local puddles of electrons and holes with finite densities^{39–41}. The potential of charged impurities moves the Dirac point up and down in different points of space creating alternating in space electron and hole puddles. From the perspective of reactivity, puddles increase the available electron density for electron transfer by increasing the number that overlap with vacant oxidation states of the reactant.

These effects should be more enhanced in a single layer over bi- or multi- layer graphene because the screening length of graphite⁴² is only 5 Å in the c-axis and is comparable to the interlayer distance ~ 3.4 Å. We expect similar short screening length for bi- and multi- layer graphene⁴³ and therefore ionized impurities in the underlying substrate should have a stronger correlative effect on single layer than in top layers of bi- and multi- layer graphene. Generally, the layer in direct contact with the SiO₂ substrate should be most affected by the ionized impurities. However, in the case of bi- or multi- layer graphene, it is presumably only the top layer that undergoes electron transfer chemical functionalization, and this layer should be least affected by charged impurities in the substrate.

We then explore the role of shifting in Dirac point of single graphene sheet due to electron hole puddles. We realize that reactivity of the single graphene sheet significantly increases by downshift of the Dirac point. Reactivity of single graphene sheet is almost three times that of a bilayer if the Dirac point downshifts by 500meV. This is due to increase in the overlap of electronic DOS of graphene and vacant oxidation states of the 4-nitrobenzene diazonium tetrafluoroborate. Therefore we expect the contribution of the ionized impurities on SiO₂ substrate for substantially increasing the on chip reactivity of single graphene sheet towards electron transfer chemistries. (Details of the calculation present in the supplement). An electron puddle has a corresponding hole puddle if charge density remains constant. The hole puddle should have reduced reactivity due to similar arguments as those above. We neglect the reduced reactivity of the hole puddle, since all that is required for increased reactivity is for a transient perturbation in charge density to result in a lowering of the Dirac point in energy.

Another possible explanation is the existence of mechanical ripples in the graphene sheet. Simulation of chemical activity of corrugated graphene within density functional theory predicts an enhancement of its chemical activity if the ratio of height of the corrugation (ripple) to its radius is larger⁴⁴ than 0.07. According to these simulations growth of the curvature of the ripples results in appearance of midgap states which leads to increase of chemisorption energy. For suspended graphene layers a single layer has been found to be more microscopically corrugated than a bi or multi- layer^{45,46}. The relevance of this phenomenon on the reactivity of graphene requires further study.

Electron transfer chemistry for graphene edges and bulk

A very important goal for the graphene community remains to develop precise control of the chemistry at graphene edges as discussed above. Edges are of particular interest since their orientations determine the electronic properties of graphene nanoribbons. Cançado et al⁴⁷ have suggested that a perfect zigzag edge cannot activate the D peak due to momentum conservation. Later Casiraghi et al⁴⁸ performed a detailed Raman spectroscopy analysis of graphene edges and according to them this dependence of D peak on the edge orientation has not been observed for real graphene samples with macroscopically smooth edges. This is attributed to the lack of high order of carbon atom orientation along the edges. Various Raman studies^{24,30} on pristine graphene have reported zero D peak intensity for the bulk pristine graphene (graphene with no edge component) due to high crystallinity and absence of defects. However, the edges exhibit finite D peak intensity since they act as defects and allow elastic backscattering of electrons. As expected, the D peak intensity of graphene and graphite edges show a strong dependence on the polarization of incident light^{47,48}. It is strongest for polarization parallel to the edge and minimum for perpendicular.

In this work, we observe a higher reactivity of graphene edges than the central interior of a single graphene sheet as presented in the schematic cartoon of figure 4. To study this observation to a greater extent, we developed a new spectroscopic test to examine the relative reactivity of graphene edges versus the interior sheet, using the polarization of various contributions to the symmetry disallowed two phonon mode (D peak) observable in the Raman spectrum of graphene edges. This polarization dependence of the intensity of this mode (D peak) for graphene and graphite edges is well documented^{47,48}.

To study the reactivity of graphene edges, we examine a procedure whereby the spatial contributions of the D peak are deconvolved and related to reactive state. By examination of the D peak intensity on the polarization of incident light before and after chemical functionalization, the contribution due to the symmetry breaking from the edge can be subtracted.

For unfunctionalized samples, the D peak at the edges of the sheet shows a strong dependence on the direction of polarization of incident light. However this dependence is invariably lost after functionalization (figure 6) indicating that the main contribution to the larger peak D peak is from the newly introduced defects introduced by attachment of functional groups. Because a 2–3 times higher D peak at the edges is observed over the bulk, we interpret this as higher reactivity of the former over the latter (figure 5)⁴⁹.

It is possible that conditions may be found where the difference in reaction rates between bulk and edge leads to exclusive reaction of the latter, an important goal in graphene processing. This may provide a direct handle to control the non-uniformity of edges for graphene and its nano ribbons. Figure 5a is the microscopic image of a graphene sheet that is single at the bottom portion. The Raman spectra of bulk (spot A1) and edges (A2) of single graphene sheet before (labeled pristine) and after (labeled functionalized) the electron transfer chemistry are presented in figure 5b and c respectively. We see no D peak for the pristine bulk single graphene (A1) and a D/G ratio of 0.1 for the edge A2. After attachment of the chemical moieties we observe much higher D/G peak ratios for the edges than for the

bulk of single sheets. For the edge (A2) D/G ratio is 0.764 and for bulk (A1) it is 0.417. This higher ratio suggests a higher reactivity of carbon atoms along and close to the edges than in the bulk. We further investigate the dependence of the D peak on incident light polarization (figure 6). The D peak for pristine graphene edge (spot E in figure 6a) shows a strong dependence on the incident light polarization. The angle between the incident polarization and the edge direction is defined as θ . The D-band is strongest for polarization parallel to the edge ($\theta=0^\circ$) and minimum for perpendicular ($\theta=90^\circ$) as shown in figure 6b. The D/G ratio is 0.12 for $\theta=0^\circ$ and is almost 0 for $\theta=90^\circ$. This dependence has been previously well studied by other researchers and is attributed to the broken symmetry of the graphene structure at edges. However, post chemical functionalization this dependence of D peak on the incident light polarization is lost for the edges. Figure 6c shows a clear indication of the isotropic D peak that is independent of the incident angle of polarization at edge E. Similar data points are presented in table T1. The bulk of graphene sheets show no D peak dependence on the angle of polarization of the incident light. To rule out the interpretation that edges might simply have higher D peaks than in the bulk for the same level of functionalization we obtained the Raman spectra of the edge and bulk of graphene oxide. We prepared graphene oxide from graphite by Hummers method⁵⁰. We expect the intensive oxidation involved in this method to fully functionalize graphene edges and bulk. The Raman spectra of these graphene oxide sheets show insignificant variation in D/G ratio of edges and bulk (figure S3) indicating no enhanced D peak for edges than bulk at same level of functionalization.

Many effects can be seen to contribute to the enhanced reactivity of the edges as compared to the bulk (central) graphene. An altered electronic structure is expected at the edges than at the bulk region due to symmetry breaking of the honeycomb lattice at the edges. For edges higher electronic DOS near Fermi level than bulk graphene is suggested by previous STM analysis⁵¹. The dangling bonds at the edges can also be a major contribution to the enhanced edge reactivity.

Independent Analysis of Chemical Functionalization—To collect more evidence of the electron transfer chemistry we perform Auger electron spectroscopy and Time-of-Flight Secondary Ion Mass Spectrometry (TOF-SIMS) on reacted graphene sheets as presented in figure 7 and 8 respectively. Auger analysis is done on a single graphene sheet ($N=1$) after electron transfer chemistry. Figure 7a,b shows the microscopic and SEM image respectively of the graphene sheet. In figure 7a the lower portion of the graphene sheet is single while the entire sheet in figure 7b is single. The Auger electron spectroscopy analysis of the boxed region in figure 7a,b with $5\mu\text{m} \times 5\mu\text{m}$ analysis area is presented in figure 7c. Analysis shows the presence of nitrogen and oxygen on the single sheet. This indicates successful attachment of the $\text{C}_6\text{H}_4\text{-NO}_2$ groups to the single graphene sheet⁵². TOF-SIMS also indicates similar results and are presented in figure 8. This analysis is only restricted to the outermost (1–2) atomic layers of the sample. TOF-SIMS is performed on multi-layer graphene sheets after their functionalization. The scan sizes are either 100 or 200 μm . The negative ion spectrum show presence of ions CN^- ($m/z=26$), NO_2^- ($m/z=42$) and CNO^- ($m/z=46$) clearly indicating attachment of $\text{C}_6\text{H}_4\text{-NO}_2$ groups on the graphene sheet.⁵³

Methods

Auger spectroscopy

PHI 700 Auger Nanoprobe instrument is used with electron beam energy of 10 kV, and 10nA of beam current.

TOF-SIMS analysis

Measurements are done with a PHI TRIFT III instrument. A primary beam of 22kV Au⁺ with a 2.4nA dc current is used. This is run in an unbunched mode to get better lateral resolution in the images. The scan sizes are either 100 or 200 microns. No charge compensation is used to collect the data. The mass range collected is 0–2000 amu and the collection time is 10 minutes. Data presented above has only the region of interest.

Conclusions

In conclusion, we have explored the reactivity of graphene and its various multi- layers for electron transfer chemistry with 4-nitrobenzene diazonium tetrafluoroborate by Raman spectroscopy, TOF-SIMS and Auger Electron Spectroscopy after reaction on-chip. Single graphene sheets are found to be almost ten times more reactive than bi- or multi- layers of graphene according to relative disorder (D) peak in the Raman spectrum examined before and after chemical reaction. We explain this anomalous increase as an effect of electron and hole puddles whereby the Dirac point deviates spatially. Because the chemistry at the graphene edge is important for controlling its electronic properties, we have developed a new spectroscopic test to examine the relative reactivity of graphene edges versus the bulk. We show, for the first time, that reactivity of edges is at least two times higher than reactivity of the bulk single graphene sheet, as supported by theory. The differences in electron transfer rates demonstrated for the first time in this study may be important for selecting and manipulating graphitic materials on-chip.

Supplementary Material

Refer to Web version on PubMed Central for supplementary material.

Acknowledgments

The authors acknowledge funding from the 2009 U.S. Office of Naval Research Multi University Research Initiative (MURI) on Graphene Advanced Terahertz Engineering (Gate) at MIT, Harvard and Boston University. M.S.S is also grateful for a 2008 Young Investigator Program Award (YIP) from the U.S. Office of Naval Research. Raman measurements were carried out in the George R. Harrison Spectroscopy Laboratory at MIT supported by NSF-CHE 0111370 and NIH-RR02594 grants. J.H. Baik is grateful for support by a Korea Research Foundation Grant funded by the Korean Government (MOEHRD) (KRF-2007-357-D00053).

Reference

1. Novoselov KS, et al. Electric field effect in atomically thin carbon films. *Science*. 2004; 306:666–669. [PubMed: 15499015]
2. Novoselov KS, et al. Two-dimensional gas of massless Dirac fermions in graphene. *Nature*. 2005; 438:197–200. [PubMed: 16281030]

3. Zhang YB, Tan YW, Stormer HL, Kim P. Experimental observation of the quantum Hall effect and Berry's phase in graphene. *Nature*. 2005; 438:201–204. [PubMed: 16281031]
4. Novoselov KS, et al. Room-temperature quantum hall effect in graphene. *Science*. 2007; 315:1379–1379. [PubMed: 17303717]
5. Morozov SV, et al. Giant intrinsic carrier mobilities in graphene and its bilayer. *Physical Review Letters*. 2008; 100
6. Bolotin KI, Sikes KJ, Hone J, Stormer HL, Kim P. Temperature-dependent transport in suspended graphene. *Physical Review Letters*. 2008; 101
7. Zhang YB, et al. Direct observation of a widely tunable bandgap in bilayer graphene. *Nature*. 2009; 459:820–823. [PubMed: 19516337]
8. Li XL, Wang XR, Zhang L, Lee SW, Dai HJ. Chemically derived, ultrasoft graphene nanoribbon semiconductors. *Science*. 2008; 319:1229–1232. [PubMed: 18218865]
9. Geim AK, Novoselov KS. The rise of graphene. *Nature Materials*. 2007; 6:183–191. [PubMed: 17330084]
10. Charlier JC, Eklund PC, Zhu J, Ferrari A. C. Electron and phonon properties of graphene: Their relationship with carbon nanotubes. 2008
11. Boukhvalov DW, Katsnelson MI. Tuning the gap in bilayer graphene using chemical functionalization: Density functional calculations. *Physical Review B*. 2008; 78
12. Zanella I, Guerini S, Fagan SB, Mendes J, Souza AG. Chemical doping-induced gap opening and spin polarization in graphene. *Physical Review B*. 2008; 77
13. Cervantes-Sodi F, Csanyi G, Piscanec S, Ferrari AC. Edge-functionalized and substitutionally doped graphene nanoribbons: Electronic and spin properties. *Physical Review B*. 2008; 77
14. Gunlycke D, Li J, Mintmire JW, White CT. Altering low-bias transport in zigzag-edge graphene nanostrips with edge chemistry. *Applied Physics Letters*. 2007; 91
15. Sharma S, Nair N, Strano MS. Structure-Reactivity Relationships for Graphene Nanoribbons. *Journal of Physical Chemistry C*. 2009
16. Niimi Y, et al. Scanning tunneling microscopy and spectroscopy of the electronic local density of states of graphite surfaces near monoatomic step edges. *Physical Review B*. 2006; 73
17. Ritter KA, Lyding JW. The influence of edge structure on the electronic properties of graphene quantum dots and nanoribbons. *Nature Materials*. 2009; 8:235–242. [PubMed: 19219032]
18. Huang JY, et al. In situ observation of graphene sublimation and multi-layer edge reconstructions. *Proceedings of the National Academy of Sciences of the United States of America*. 2009; 106:10103–10108. [PubMed: 19515820]
19. Lomeda JR, Doyle CD, Kosynkin DV, Hwang WF, Tour JM. Diazonium Functionalization of Surfactant-Wrapped Chemically Converted Graphene Sheets. *Journal of the American Chemical Society*. 2008; 130:16201–16206. [PubMed: 18998637]
20. Bekyarova E, et al. Chemical Modification of Epitaxial Graphene: Spontaneous Grafting of Aryl Groups. *Journal of the American Chemical Society*. 2009; 131:1336. [PubMed: 19173656]
21. Schniepp HC, Saville DA, Aksay IA. Self-healing of surfactant surface micelles on millisecond time scales. *Journal of the American Chemical Society*. 2006; 128:12378–12379. [PubMed: 16984163]
22. Usrey ML, Lippmann ES, Strano MS. Evidence for a two-step mechanism in electronically selective single-walled carbon nanotube reactions. *Journal of the American Chemical Society*. 2005; 127:16129–16135. [PubMed: 16287300]
23. Casiraghi C, et al. Rayleigh imaging of graphene and graphene layers. *Nano Letters*. 2007; 7:2711–2717. [PubMed: 17713959]
24. Ferrari AC, et al. Raman spectrum of graphene and graphene layers. *Physical Review Letters*. 2006; 97
25. Souza AG, et al. Strain-induced interference effects on the resonance Raman cross section of carbon nanotubes. *Physical Review Letters*. 2005; 95
26. Cronin SB, et al. Measuring the uniaxial strain of individual single-wall carbon nanotubes: Resonance Raman spectra of atomic-force-microscope modified single-wall nanotubes. *Physical Review Letters*. 2004; 93

27. Rao AM, Eklund PC, Bandow S, Thess A, Smalley RE. Evidence for charge transfer in doped carbon nanotube bundles from Raman scattering. *Nature*. 1997; 388:257–259.
28. Casiraghi C, Pisana S, Novoselov KS, Geim AK, Ferrari AC. Raman fingerprint of charged impurities in graphene. *Applied Physics Letters*. 2007; 91
29. Pisana S, et al. Breakdown of the adiabatic Born-Oppenheimer approximation in graphene. *Nature Materials*. 2007; 6:198–201. [PubMed: 17293849]
30. Ferrari AC. Raman spectroscopy of graphene and graphite: Disorder, electron-phonon coupling, doping and nonadiabatic effects. *Solid State Communications*. 2007; 143:47–57.
31. Das A, et al. Monitoring dopants by Raman scattering in an electrochemically top-gated graphene transistor. *Nature Nanotechnology*. 2008; 3:210–215.
32. Ferralis N, Maboudian R, Carraro C. Evidence of Structural Strain in Epitaxial Graphene Layers on 6H-SiC(0001). *Physical Review Letters*. 2008; 101
33. Mohiuddin TMG, et al. Uniaxial strain in graphene by Raman spectroscopy: G peak splitting, Gruneisen parameters, and sample orientation. *Physical Review B*. 2009; 79
34. Fantini C, Pimenta MA, Strano MS. Two-phonon combination Raman modes in covalently functionalized single-wall carbon nanotubes. *Journal of Physical Chemistry C*. 2008; 112:13150–13155.
35. Gerischer, H. *Physical Chemistry: An Advanced Treatise*. Eyring, H, editor. New York: Academic Press, Inc; 1970.
36. Nair N, Kim WJ, Usrey ML, Strano MS. A structure-reactivity relationship for single walled carbon nanotubes reacting with 4-hydroxybenzene diazonium salt. *Journal of the American Chemical Society*. 2007; 129:3946–3954. [PubMed: 17352473]
37. Ando T. Anomaly of optical phonons in bilayer graphene. *Journal of the Physical Society of Japan*. 2007; 76
38. Charlier JC, Gonze X, Michenaud JP. First-principles study of stacking effect on the electronic properties of graphite(s). *Carbon*. 1993; 32:289–299.
39. Hwang EH, Adam S, Das Sarma S. Carrier transport in two-dimensional graphene layers. *Physical Review Letters*. 2007; 98
40. Galitski VM, Adam S, Das Sarma S. Statistics of random voltage fluctuations and the low-density residual conductivity of graphene. *Physical Review B*. 2007; 76
41. Shklovskii BI. Simple model of Coulomb disorder and screening in graphene. *Physical Review B*. 2007; 76
42. Pietronero L, Strassler S, Zeller HR, Rice MJ. Charge-Distribution in C Direction in Lamellar Graphite Acceptor Intercalation Compounds. *Physical Review Letters*. 1978; 41:763–767.
43. Lin YM, Avouris P. Strong suppression of electrical noise in bilayer graphene nanodevices. *Nano Letters*. 2008; 8:2119–2125. [PubMed: 18298094]
44. Boukhvalov, DW, Katsnelson, MI. arXiv:0905.2137. 2009. Enhancement of chemical activity in corrugated graphene.
45. Meyer JC, et al. The structure of suspended graphene sheets. *Nature*. 2007; 446:60–63. [PubMed: 17330039]
46. Meyer JC, et al. On the roughness of single- and bi-layer graphene membranes. *Solid State Communications*. 2007; 143:101–109.
47. Cancado LG, Pimenta MA, Neves BRA, Dantas MSS, Jorio A. Influence of the atomic structure on the Raman spectra of graphite edges. *Physical Review Letters*. 2004; 93
48. Casiraghi C, et al. Raman Spectroscopy of Graphene Edges. *Nano Letters*. 2009; 9:1433–1441. [PubMed: 19290608]
49. The D/G peak in figure 5 is almost two time higher than in Figure 2. This is due to the longer reaction time (~12hours) and higher temperature
50. Li D, Muller MB, Gilje S, Kaner RB, Wallace GG. Processable aqueous dispersions of graphene nanosheets. *Nature Nanotechnology*. 2008; 3:101–105.
51. Klusek Z, et al. Local electronic edge states of graphene layer deposited on IR111) surface studied by STM/CITS. *Applied Surface Science*. 2005; 252:1221–1227.

52. Some contribution of oxygen is also from SiO₂ below due to the very small thickness of single graphene sheet. For this reason Si is also seen in Auger analysis for single sheets. To confirm that oxygen is also present on the graphene sheets (i.e C₆H₄-NO₂) we did Auger from multi layer graphene sheets for which we saw no Si signal. For these multi layer graphene samples also we saw O indicating its presence in the groups reacted to the graphene sheets.
53. 80 and 97 peaks are due to SO₃⁻ and HSO₄⁻ respectively. These come from the sulfur in SDS. SDS residue remains on the graphene surface in very small amount. However, TOF-SIMS is very sensitive to presence of sulfur since it is easy to ionize it unlike nitrogen that is harder to ionize.

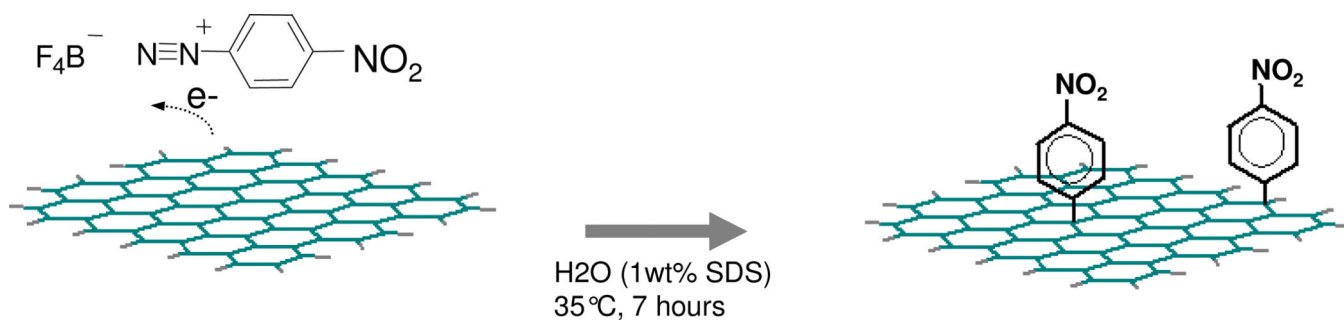


Figure 1.
Schematic of the electron transfer chemistry between graphene and 4 nitro benzene diazonium tetrafluoroborate.

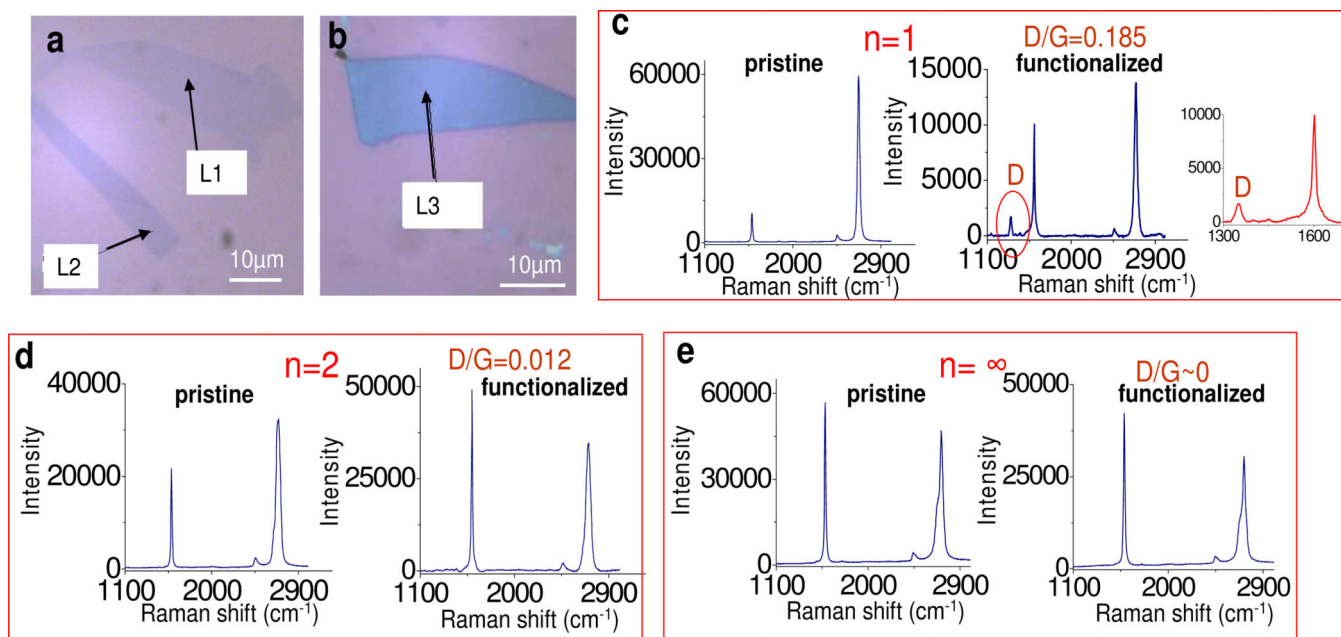


Figure 2.

(a) Microscopic images of a single layer (right), bilayer (left) and (b) multilayer ($n \sim \infty$) of graphene. (c–e) Raman spectra of pristine (left) and functionalized (right) sheets: (c) spot L1 on single sheet with inset showing expanded 1300–1700 cm^{-1} region, (d) spot L2 on bilayer and (e) spot L3 on multilayer ($n \sim \infty$, graphite). There is no D peak for the pristine samples (left spectra). The D/G ratio after reaction of single layer (0.185) is about 15 times higher than for a bilayer (0.012) and greater for other multilayers (~ 0). Reactions are all performed at 35 °C with 17 mM 4-nitrobenzene diazonium water with 1 wt% SDS.

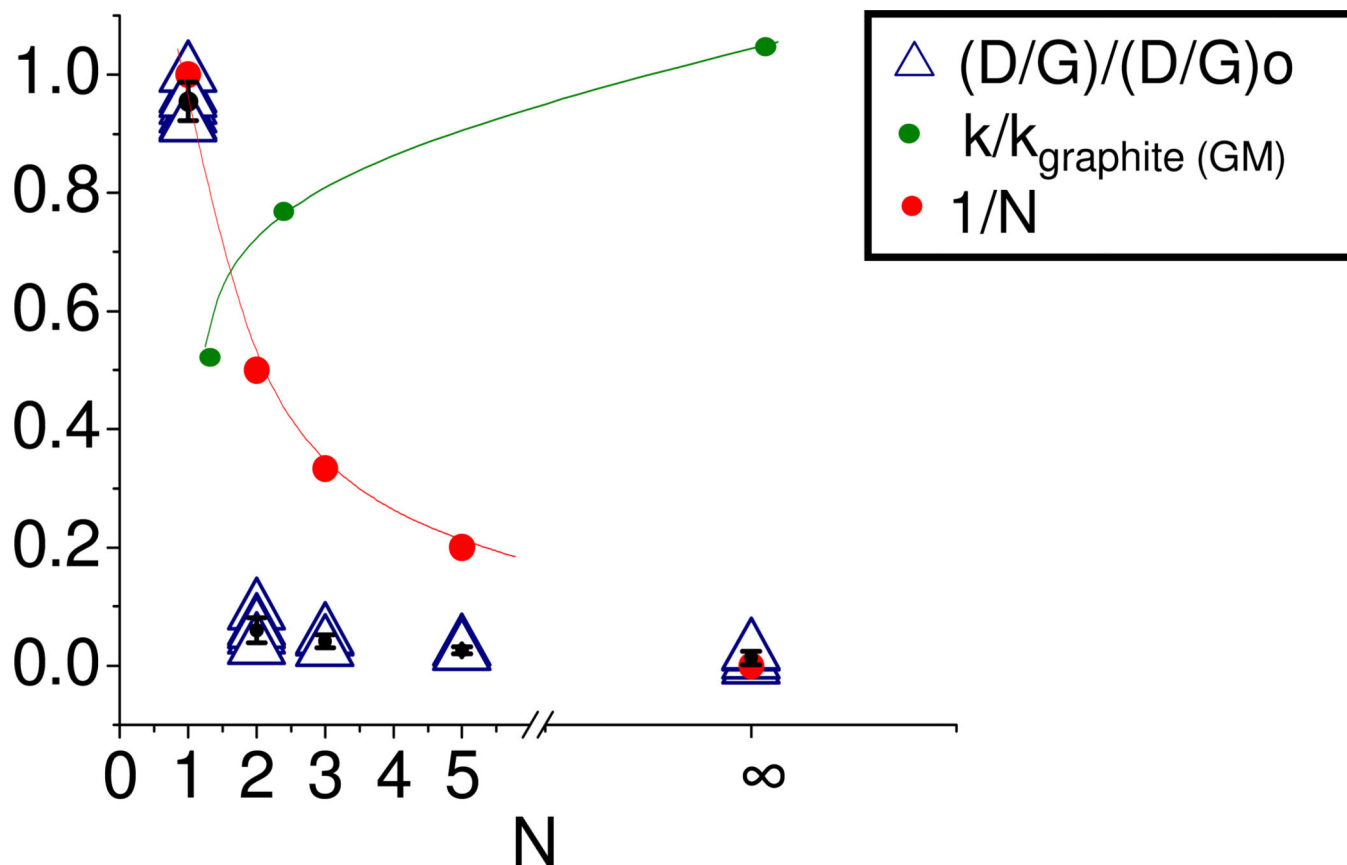


Figure 3.

Dependence of D/G peak ratio, normalized to the maximum value encountered on the substrate, on the number of graphene layers (N). The data set combines results from graphene sheets from multiple silicon substrates. (N=∞ corresponds to graphite). 1/N (red) represents the expected D/G scaling with N if the topmost graphene sheets of multilayers have the same reactivity as that of single sheet. Calculations (green) of the reactivity normalized to graphite k/k_{graphite} for the case of no electronic puddles using Gerischer Marcus theory.

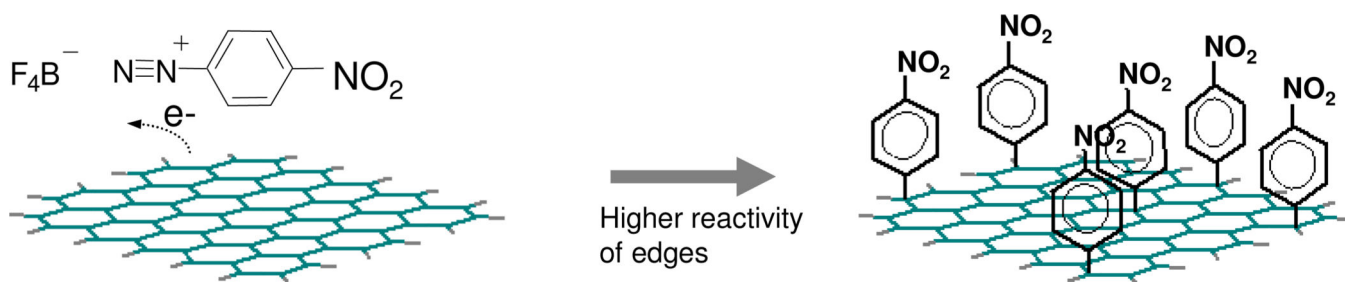


Figure 4. Higher edge reactivity. The number density of functional groups $\text{C}_6\text{H}_4\text{-NO}_2$ is higher at the edges of graphene than at the bulk.

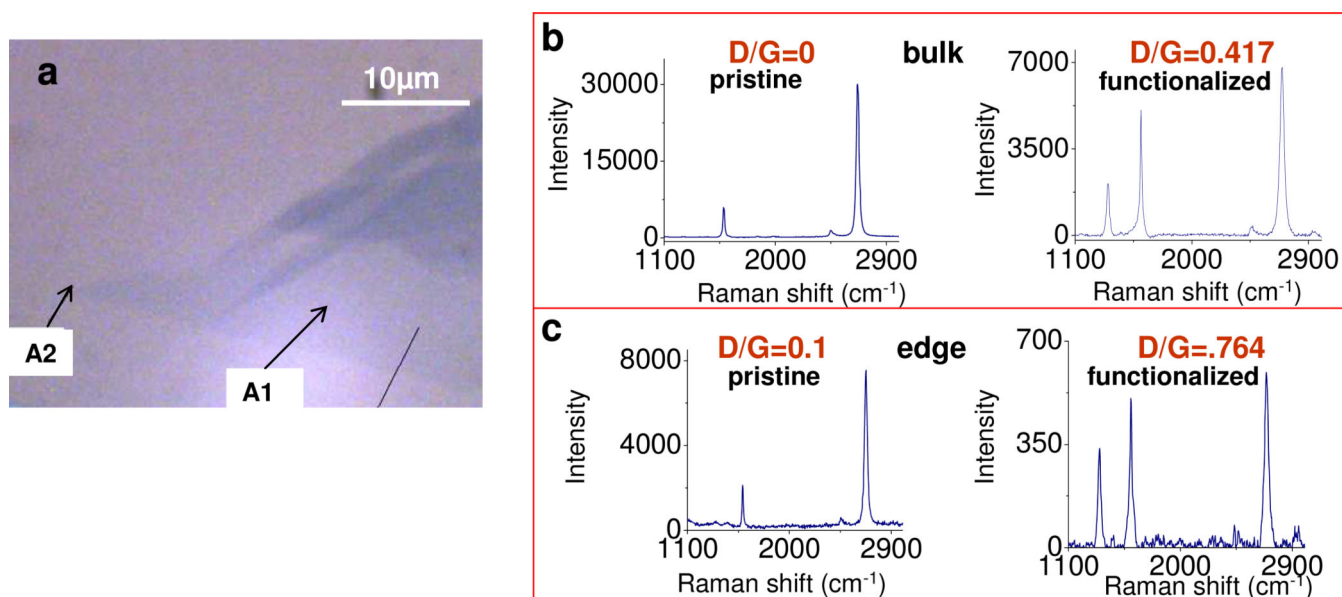


Figure 5.

The graphene edges show markedly higher reactivity. (a) Microscopic image of a graphene sheet with lower portion (lighter color) as single and upper (darker) is 2–3 layers. (b) Raman spectra of A1 (point on bulk single graphene) and c) A2 (point on the edge of single graphene) before (pristine) and after electron transfer chemistry (functionalized). Note that D/G ratio is 0 for bulk (A1) and 0.1 for edge (A2) before chemistry but rises to 0.417 and 0.764 after reaction for the bulk and edge contribution respectively for a single sheet, absent polarized filtering. Reactions are all performed at 45 °C with 25 mM 4-nitrobenzene diazonium water with 1 wt% SDS.

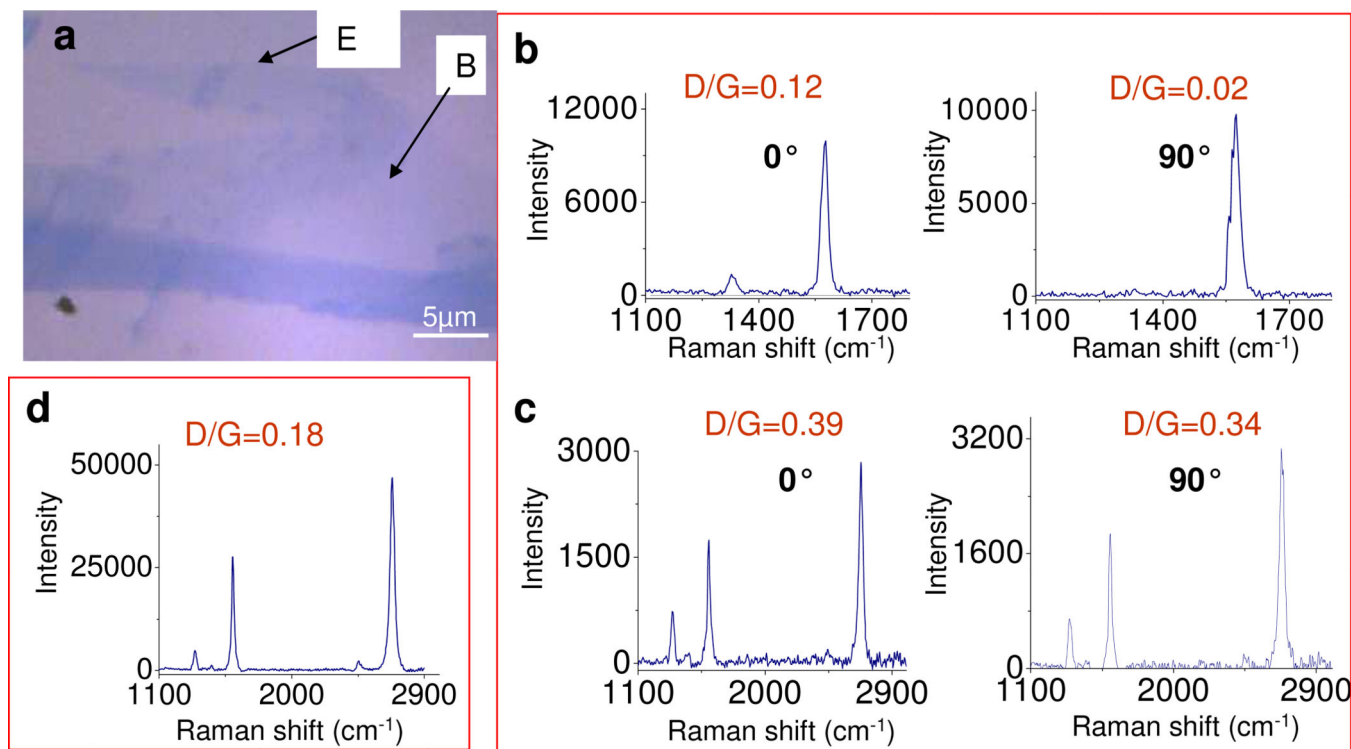


Figure 6. Polarization dependence of D peak before and after electron transfer chemistry. (a) Microscopic image of graphene sheet. The upper part is a single layer. (b) Raman of pristine graphene sheet edge (spot E): D peak depends on the angle of polarization of the incident laser light. Light parallel to the edge is 0° and perpendicular is 90°. The D/G=0.12 for 0° but 0.02 for 90° for edge of pristine sheet. (c) Edge point E after reaction shows weak or no dependence of D peak on the angle of polarization. (d) Point on the bulk of single graphene sheet has a lower D/G than edge and no polarization dependence. Reactions are all performed at 35 °C with 17 mM 4-nitrobenzene diazonium water with 1 wt% SDS.

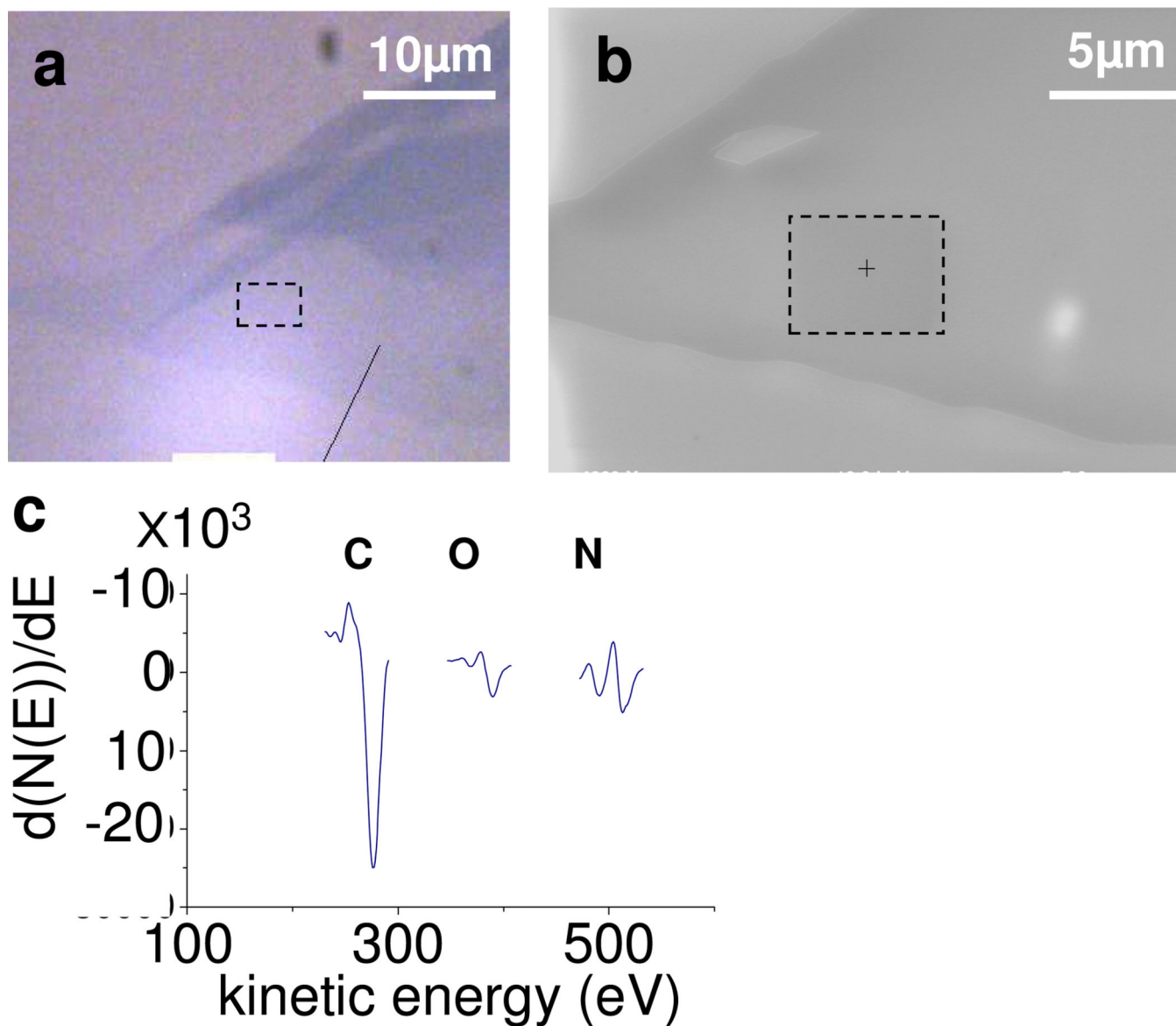


Figure 7. Auger Electron Spectroscopy analysis of single graphene sheet ($5 \mu\text{m} \times 5 \mu\text{m}$ analysis area) after electron transfer chemistry. **(a)** Microscopic image of graphene sheet. Bottom part is a single sheet and upper portion has 2–3 layers of graphene sheets. The dashed box marks the area for AUGER analysis. **(b)** SEM analysis done during AUGER analysis on the single graphene layer portion in (a). Dashed box highlights the area ($5 \mu\text{m} \times 5 \mu\text{m}$) of AUGER analysis. **(c)** Nitrogen (N) indicates successful attachment of $\text{C}_6\text{H}_4\text{-NO}_2$ to the single sheets. O has contributions from both SiO_2 and NO_2 groups.

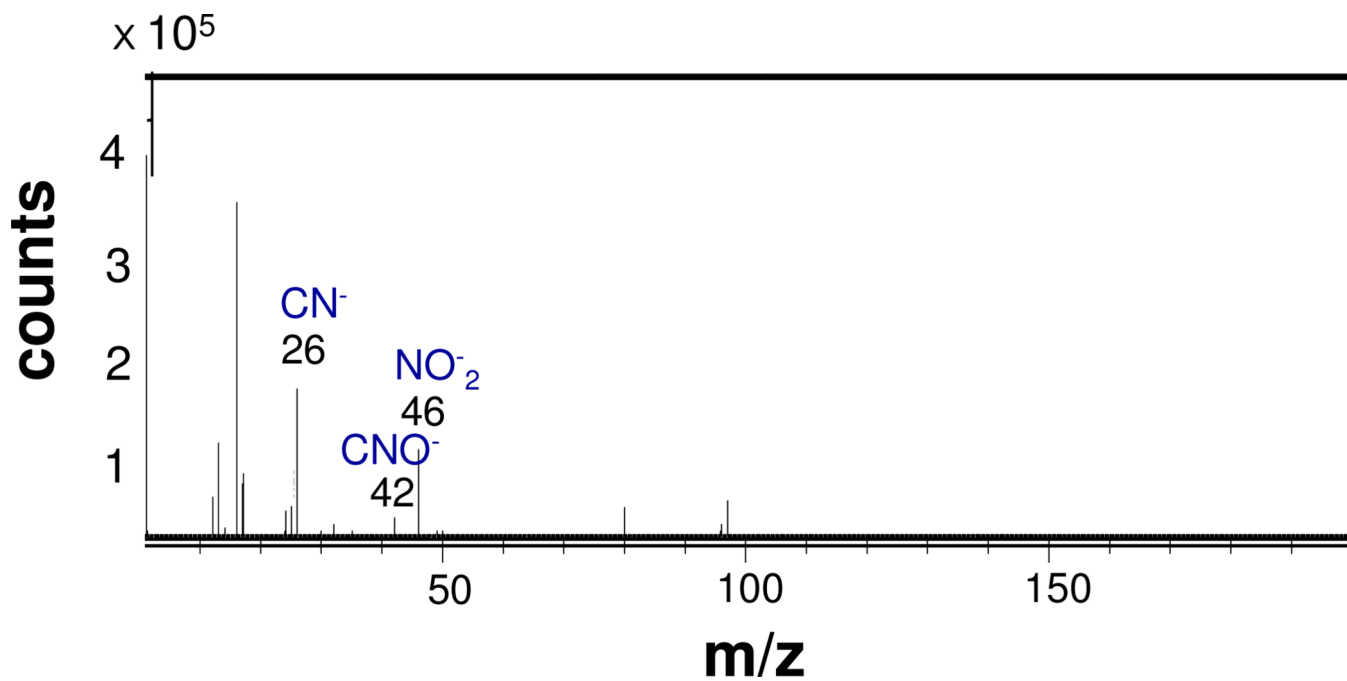


Figure 8.

TOF-SIMS (negative ion) spectrum of multilayer graphene sheets after electron transfer chemistry. TOF-SIMS analysis is only restricted to the outermost (1–2) atomic layers of the sample. In the on chip electron transfer chemistry only the topmost graphene sheet is functionalized with the nitro diazonium salt. Presence of signal corresponding to CN^- ($m/z=26$), CNO^- ($m/z=42$), and NO_2^- ($m/z=46$), confirms successful attachment of $\text{C}_6\text{H}_4\text{-NO}_2$ group to the topmost graphene layer.

Table T1

Dependence of D peak of edges on the angle of polarization after functionalization. The first three data points correspond to 4-nitrobenzene diazonium tetrafluoroborate and fourth corresponds to 3–5-dichlorophenyl diazonium tetrafluoroborate as the chemical moieties reacting with graphene.

D/G (incident light parallel to graphene edge)	D/G (incident light perpendicular to graphene edge)
0.375	0.31
0.35	0.34
0.39	0.34
0.278	0.226

Author Manuscript

Author Manuscript

Author Manuscript

Author Manuscript